



Article

Prediction of Multi-Site PM_{2.5} Concentrations in Beijing Using CNN-Bi LSTM with CBAM

Dong Li ^{1,2,3,4}, Jiping Liu ² and Yangyang Zhao ^{2,*}

¹ Faculty of Geomatics, Lanzhou Jiaotong University, Lanzhou 730070, China

² Chinese Academy of Surveying and Mapping, Beijing 100830, China

³ National-Local Joint Engineering Research Center of Technologies and Applications for National Geographic State Monitoring, Lanzhou 730070, China

⁴ Gansu Provincial Engineering Laboratory for National Geographic State Monitoring, Lanzhou 730070, China

* Correspondence: zhaoyy@casm.ac.cn

Abstract: Air pollution is a growing problem and poses a challenge to people's healthy lives. Accurate prediction of air pollutant concentrations is considered the key to air pollution warning and management. In this paper, a novel PM_{2.5} concentration prediction model, CBAM-CNN-Bi LSTM, is constructed by deep learning techniques based on the principles related to spatial big data. This model consists of the convolutional block attention module (CBAM), the convolutional neural network (CNN), and the bi-directional long short-term memory neural network (Bi LSTM). CBAM is applied to the extraction of feature relationships between pollutant data and meteorological data and assists in deeply obtaining the spatial distribution characteristics of PM_{2.5} concentrations. As the output layer, Bi LSTM obtains the variation pattern of PM_{2.5} concentrations from spatial data, overcomes the problem of long-term dependence on PM_{2.5} concentrations, and achieves the task of accurately forecasting PM_{2.5} concentrations at multiple sites. Based on real datasets, we perform an experimental evaluation and the results show that, in comparison to other models, CBAM-CNN-Bi LSTM improves the accuracy of PM_{2.5} concentration prediction. For the prediction tasks from 1 to 12 h, our proposed prediction model performs well. For the 13 to 48 h prediction task, the CBAM-CNN-Bi LSTM also achieves satisfactory results.



Citation: Li, D.; Liu, J.; Zhao, Y.

Prediction of Multi-Site PM_{2.5}

Concentrations in Beijing Using CNN-Bi LSTM with CBAM.

Atmosphere **2022**, *13*, 1719. <https://doi.org/10.3390/atmos13101719>

Academic Editor: Antonio Donato

Received: 8 September 2022

Accepted: 14 October 2022

Published: 19 October 2022

Publisher's Note: MDPI stays neutral with regard to jurisdictional claims in published maps and institutional affiliations.



Copyright: © 2022 by the authors. Licensee MDPI, Basel, Switzerland. This article is an open access article distributed under the terms and conditions of the Creative Commons Attribution (CC BY) license (<https://creativecommons.org/licenses/by/4.0/>).

1. Introduction

Over the past few years, significant social concern has been generated by the increasingly serious issue of air pollution. [1]. Prediction of pollutant concentrations in the air plays an essential role in environmental management and air pollution prevention [2]. PM_{2.5} (particulate matter less than 2.5 μm in diameter) is an important component of air pollutants [3]. Therefore, the prediction of PM_{2.5} concentration trends is considered a critical issue in the prediction of air pollutant concentrations.

Deterministic and statistical approaches can be used to forecast PM_{2.5} concentrations based on the features of the study methods. [4]. Deterministic methods simulate the emission, dispersion, transformation, and removal of PM_{2.5} through meteorological principles and statistical methods [5], thus enabling the prediction of PM_{2.5} concentrations. There are several representative models for pollutant concentration prediction based on deterministic methods. There are a few representative models for forecasting PM_{2.5} concentrations based on deterministic methods: a Community Multiscale Air Quality Modeling System (CMAQ) [6], a nested air quality prediction modeling system (NAQPMS) [7], and a Weather Research and Forecasting Model with Chemistry (WRF-Chem) [8].

Different from the deterministic methods, the statistical methods do not have complex theoretical models, and they give better predictions through the learning and analysis of historical data on pollutants. Statistical methods are mainly classified into two approaches:

machine learning approaches and deep learning approaches [9]. The classical machine learning models used for the prediction of PM_{2.5} concentrations include Random Forest (RF) [10] models, Autoregressive Sliding Average (ARMA) Models [11], Autoregressive Integrated Moving Average (ARIMA) Models [12], Support Vector Regression (SVR) [13], and Linear Regression (LR) models [14].

Compared with machine learning methods, which suffer from slow convergence and inadequate generalization [5], deep learning is widely used in PM_{2.5} concentration prediction due to its ability to fit data more robustly and non-linearly [15]. The following deep learning models have been used to forecast pollution concentrations: Convolutional neural networks (CNN) [16], Back Propagation Neural Networks (BPNN) [17], Recurrent Neural Networks (RNN) [18], Gate Recurrent Units (GRU) [19], Long Short-Term Memory networks (LSTM) [20], and Bi-directional Long Short-Term Memory Neural Networks (Bi LSTM) [21], attention-based ConvLSTM (Att-ConvLSTM) [22], etc. Although the above models are widely used in PM_{2.5} concentration prediction due to their superiority in handling time series data, the current pollutant concentration prediction models described above have the following problem: owing to the single network model, it is limited by the feature dimension of the input data, in other words, the dimension of the hidden state is influenced by the dimension of the input data.

In order to solve the problem that the predictive power of a single deep learning network is limited, in recent years, hybrid deep learning models have been widely used in the research of pollutant concentration prediction. Hybrid deep learning models have several different network structures that allow better quantification of complex data [23], which have been used for pollutant concentration prediction, including: LSTM-FC [24], AC-LSTM [25], EEMD-GRNN [26], etc. Meanwhile, air pollution is a problem of regional dispersion with spatial dimensions [27], and there is a spatial interrelationship of air pollution between adjacent sites. However, all of the above hybrid deep learning models have focused on the prediction of pollutant concentrations at individual stations and have not considered the spatial correlation of adjacent observation sites. CNN-LSTM [15] is a recently proposed hybrid deep learning model, which can handle time series problems and has successfully interpreted the spatial distribution characteristics of air pollutant concentrations through the image analysis capability of CNN [15]. However, there are also three crucial problems with CNN-LSTM [28]. Firstly, the simple structure of CNN leads to the loss of feature information and the inability to extract deep spatial features of contaminant data [29]. Secondly, CNN-LSTM has difficulty capturing the long time-series variation between pollutant concentrations. Finally, much of the work at the present stage confirms the complex interactions between pollutant data and meteorological data [5]. CNN-LSTM has trouble obtaining complicated correlation characteristics between meteorological input and air pollution input. In view of the above, we introduced the convolutional block attention module (CBAM) to build a CNN-based prediction model: the CBAM-CNN-Bi LSTM model. The reasons are as follows.

- (1) The convolutional block attention module includes the channel attention module (CAM) and the spatial attention module (SAM) [30]. It is a simple and effective attention module that can be arbitrarily embedded into any 2D CNN model and does not consume too much of the computer's running memory.
- (2) As the network depth is increased, convolutional neural networks degrade and lose feature information. Therefore, we introduce a spatial attention module to efficiently extract spatially relevant features of contaminant data between multiple stations [29].
- (3) The correlation characteristics between pollution data and meteorological data are not taken into account by the aforementioned prediction models. In order to optimize the prediction outcomes based on the intricate correlation characteristics of the model input data, we thoroughly analyze the prediction problems of pollution data and meteorological data at each station and present the channel attention module.

In this study, our proposed prediction model is fully taken into account to produce more accurate predictions of PM_{2.5} concentrations in the target city in the future, which

should achieve the following goals: (1) efficiently utilizing historical pollutant concentration and meteorological big data from multiple stations; (2) accurately achieving long-term predictions of pollutant concentrations in the target city; and (3) in-depth exploration of the spatial and temporal correlation characteristics from multiple stations.

The remainder of the essay is structured as follows. The study area, the experimental data and the procedures for processing the experimental data, as well as the overall framework of the pollutant concentration prediction model, and a detailed explanation of each model component are described in Section 2. The key findings and expectations are covered in Section 3. The work is concluded in Section 4, which also suggests areas for future investigation.

2. Materials and Methods

2.1. Materials

2.1.1. Data

The experimental information in this study consists of pollutant data and meteorological data. The data was monitored by twelve air quality monitoring stations in the Beijing area from 1 March 2013 to 28 February 2017. The distribution of the twelve stations is shown in Figure 1a. The meteorological data and pollutant data selected are from the UCI website (<https://archive.ics.uci.edu/ml/datasets/Beijing+Multi-Site+Air-Quality+Data>, accessed on 1 April 2022). Figure 1b shows a time series plot of PM_{2.5} concentration data from twelve stations for the period 1–31 December 2016. The meteorological data include hourly temperature, pressure, dew point, precipitation, wind direction, and wind speed; and the pollutant data include hourly PM_{2.5}, PM₁₀, SO₂, NO₂, CO, and O₃. Table 1 shows the range of values for meteorological data and pollutant data.

Table 1. Experimental data of the PM_{2.5} concentration prediction model.

Type	Variable	Unit
Meteorological Data	Temperature	[−19.9, 41.6]
	Pressure	[982.4, 1042.8]
	Dew Point	[−43.4, 29.1]
	Precipitation	[0, 72.5]
	Wind Direction	[N, ESE]
	Wind Speed	[0, 13.2]
Pollutant Data	PM _{2.5}	[2, 999]
	PM ₁₀	[2, 999]
	SO ₂	[0.2856, 500]
	NO ₂	[1.0265, 290]
	CO	[100, 10000]
	O ₃	[0.2142, 1071]

2.1.2. Data Preprocessing

Wind direction, as a non-numerical type of data, needs to be converted to a numerical type of data by categorical coding. The average of the data prior to and following the time of the missing value is used to fill in missing values for meteorological and pollution data. Then, in order to eliminate the effect of numerical differences on prediction accuracy, meteorological and pollutant data were converted to the range [0, 1] by the Min-Max function as below.

$$y' = \frac{y - \min(y)}{\max(y) - \min(y)} \quad (1)$$

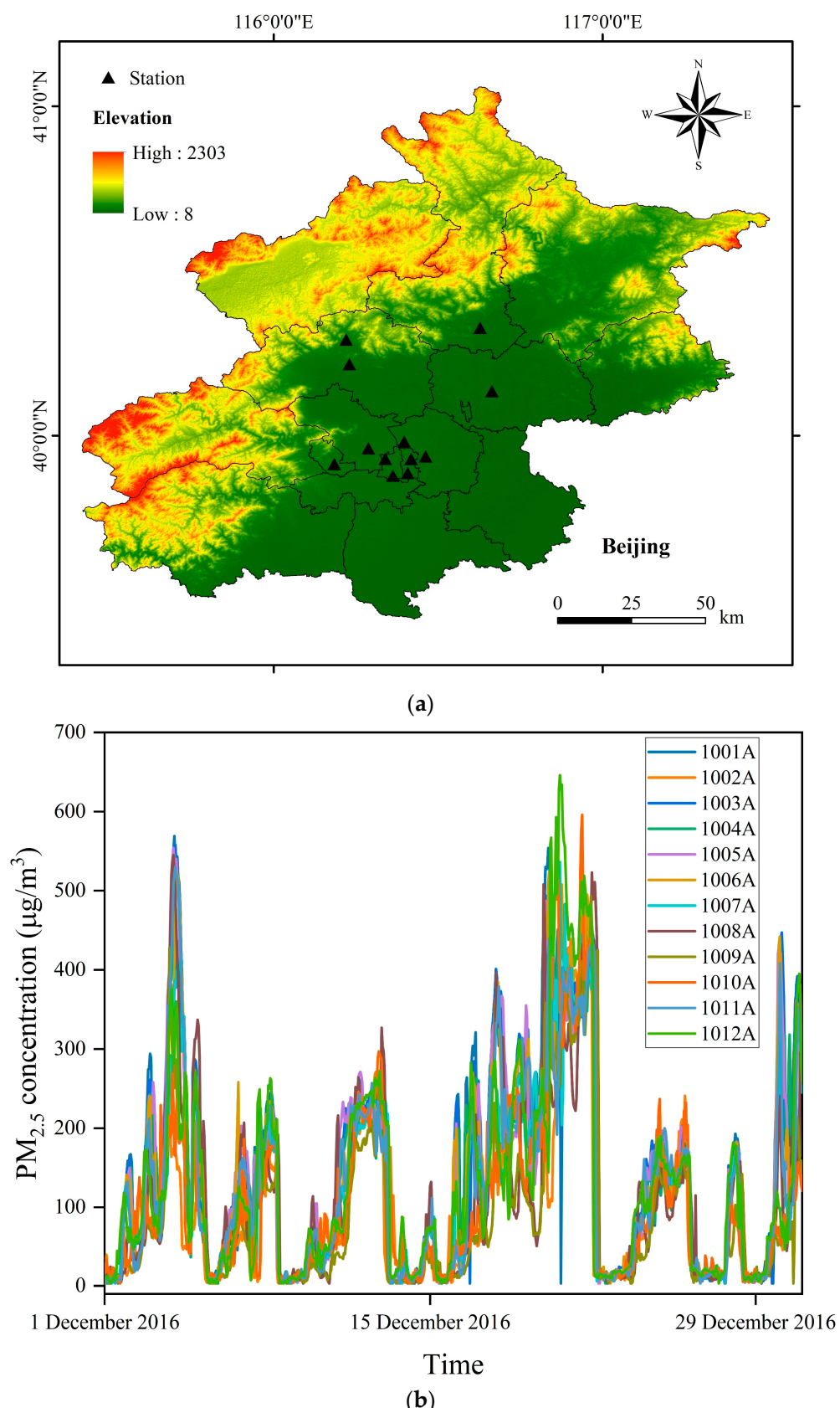


Figure 1. (a). Distribution of air quality monitoring stations in Beijing. (b). Time series plot of PM_{2.5} concentration data.

2.2. Methods

2.2.1. CBAM-CNN-Bi LSTM

Deep learning is a type of machine learning that can train samples of data using unsupervised approaches in order to create deep network structures [31]. We propose a CBAM-CNN-Bi LSTM model, whose intricate structure is depicted in Figure 2, to reliably anticipate PM_{2.5} concentrations. First, we took advantage of CNN properties to identify key characteristics in the input PM_{2.5} data and to obtain the spatial dependence of all PM_{2.5} sites. Then, we capture the time dependence of the PM_{2.5} series data using the special architecture of Bi LSTM for time-series problems. In addition, we added the convolutional block attention module to the CNN to enhance training accuracy by focusing on channel and spatial information. The convolutional block attention module is classified into the channel attention module and the spatial attention module. The channel attention module enables the network to disregard the remainder and concentrate on the useful feature channels. The spatial attention module enables the network to concentrate on the nearby areas on the feature map [32]. In other words, the channel attention module enables the network to focus on the classes of factors which have a greater impact on PM_{2.5} concentrations, and the spatial attention module enables the network to focus on areas where there is a stronger spatial relationship between PM_{2.5} sites.

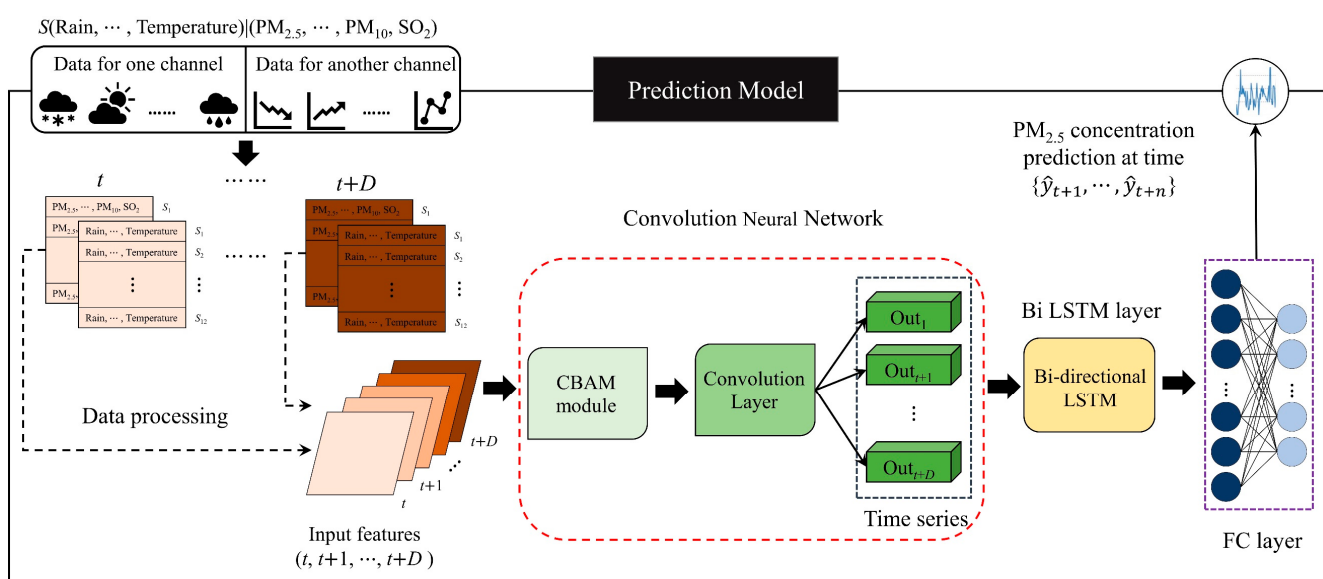


Figure 2. The architecture of CBAM-CNN-Bi LSTM.

The CNN serves as the basis layer for the CBAM-CNN-Bi LSTM model, and its convolutional layer is used to extract features. The convolutional block attention module is embedded in the CNN, and the channel and spatial feature information in the convolutional block attention module capture is used as an input for the CNN. For time series prediction, the higher layer Bi LSTM uses the output of the CNN layer as its input. In Figure 2, the prediction model is displayed.

Meteorological data and pollutant concentrations are converted into two-dimensional matrices with time series as inputs to the prediction model. These matrices are then fed into the convolutional block attention module and the CNN network in order to obtain characteristics. Its output serves as the Bi LSTM's input. The fully connected layer decodes the Bi LSTM's output to get the final prediction result.

2.2.2. Convolutional Block Attention Module

Figure 3a shows the architecture of the convolutional block attention module [33], which can perform attention in both the channel dimension and the spatial dimension

by concentrating on important elements while disregarding unimportant ones. There are two independent sub-modules in the convolutional block attention module, the channel attention module and the spatial attention module, and the structure of each of these two sub-modules is shown in Figure 3b,c. The characteristic map is created by the convolutional layer, and the weighting of the characteristic map is calculated along the order of the channel attention module first and then the spatial attention module. Then, the weight map and the input feature map are multiplied to carry out adaptive feature optimization learning [30]. The convolutional block attention module is designed as a simple attention block which is casually embedded into any 2D CNN model for end-to-end training and improved model representation at a lower cost [33].

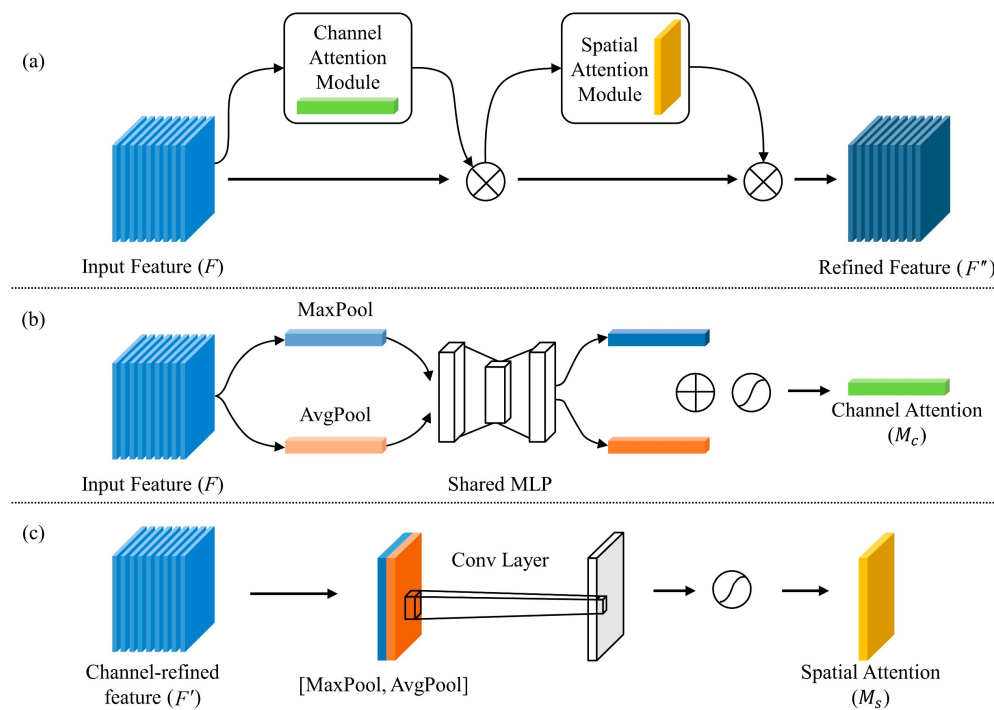


Figure 3. The architecture of convolutional block attention module. (a) The convolutional block attention module. (b) The architecture of channel attention. (c) The architecture of spatial attention. Reproduced with permission from Ref. [34]. Copyright 2021 ELSEVIER.

As shown in Figure 3a, the convolutional block attention module combines the spatial attention and channel attention modules to infer attention weight maps and produces detailed characteristic maps. These two sub-modules together are referred to as:

$$F' = M_c(F) \otimes F \quad (2)$$

$$F'' = M_s(F') \otimes F' \quad (3)$$

Here, \otimes denotes element-wise multiplication, F represents the input feature map, F' represents the channel-refined characteristic map, F'' is the refined characteristic map.

The channel attention module identifies the more important channels based on their relationship to each other. The channel attention module has two pools, *Maxpool* and *Avgpool*(·). Firstly, the input features are extracted by *Maxpool* and *Avgpool*(·) for different high-level features. By using shared MLP (multi-layer perceptron), the two categories of high-level characteristics are then combined. Lastly, a sigmoid function activates the fused features to show the channel priority of the input characteristics. The channel attention module's computation is done in the manner listed below.

$$M_c(F) = f_{sigmoid}(MLP(\text{MaxPool}(F) + MLP(\text{AvgPool}(F))) \quad (4)$$

The spatial attention module acts as a complement to the channel attention module, and it focuses on which position of information is more important. At first, *Maxpool* and *Avgpool*(·) are performed on the input features. Then, the outputs of two different features are connected to generate a novel characteristic descriptor. Lastly, the new feature descriptors are transformed into refined features through the convolution and sigmoid function operations. The following describes how the SAM is calculated.

$$M_s(F) = f_{sigmoid}(Conv[MaxPool(F); AvgPool(F)]) \quad (5)$$

where *Maxpool*(·) represents maxpooling, *Avgpool*(·) represents averagepooling, *MLP*(·) represents the multi-layer perceptron, and *Conv*(·) represents a CNN layer.

2.2.3. Convolutional Neural Network

The widely-used CNN in image analysis offers strong grid data processing capabilities [35]. As shown in Figure 4, the input, convolutional, pooling, fully connected, and output layers make up the fundamental architecture of the CNN. The convolution and pooling layers transform and extract features from the information in the input layer. The fully connected layer then performs the mapping between the resulting characteristic maps and output values [16].

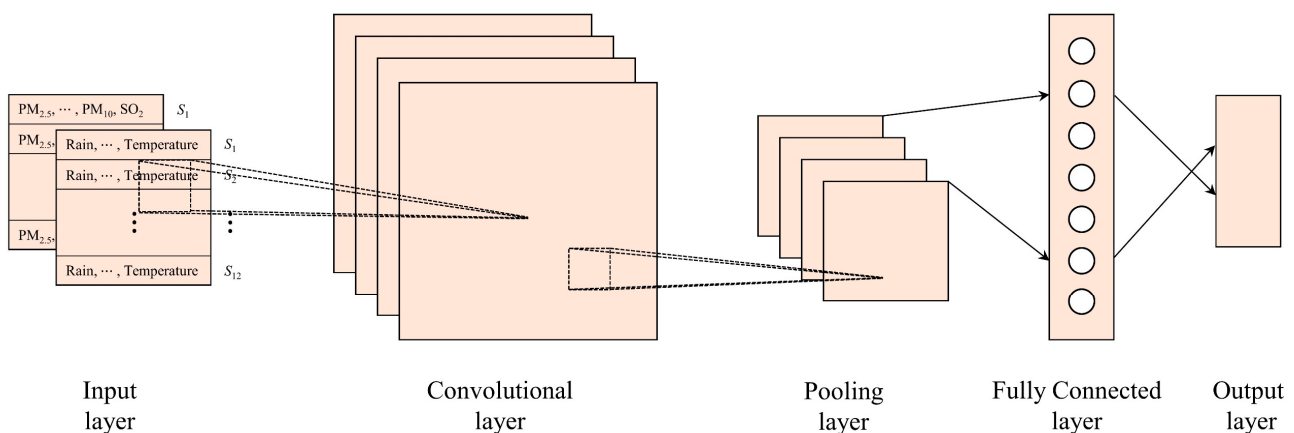


Figure 4. The fundamental architecture of CNN.

The convolutional layer, the most important layer in the CNN, extracts the features of the input image by means of the convolutional kernel. The size of the input matrix is larger than the convolution kernel. The convolution layer uses convolution operations to output the characteristic map. Each component of the feature map has the following calculation formula.

$$x_{i,j}^{out} = f_{Conv}\left(\sum_{m=0}^k \sum_{n=0}^k w_{m,n} x_{i+m,j+n}^{in} + b\right) \quad (6)$$

where $x_{i,j}^{out}$ is the characteristic map's output value for row i and column j ; $x_{i+m,j+m}^{in}$ is the value in the input matrix's row i and column j ; $f_{Conv}(\cdot)$ is activation function; $w_{m,n}$ is the convolution kernel's weight in row m and column n ; and b is the convolution kernel's bias [23].

2.2.4. Bi-Directional Long Short-Term Memory

In order to overcome the difficulty of the long-term dependence of time series data, the LSTM introduces a special cell storage structure. As shown in Figure 5b, the architecture of

each LSTM cell has an input gate i_t , a forgetting gate f_t , and an output gate O_t . The specific derivation of the LSTM is as follows.

$$f_t = \sigma(W_f \cdot [h_{t-1}, x_t] + b_f) \quad (7)$$

$$i_t = \sigma(W_i \cdot [h_{t-1}, x_t] + b_i) \quad (8)$$

$$\tilde{C}_t = \tanh(W_C \cdot [h_{t-1}, x_t] + b_C) \quad (9)$$

$$C_t = f_t * C_{t-1} + i_t * \tilde{C}_t \quad (10)$$

$$O_t = \sigma(W_o \cdot [h_{t-1}, x_t] + b_o) \quad (11)$$

$$h_t = O_t * \tanh(C_t) \quad (12)$$

where W_f , W_i , W_C , and W_o are the input weights, b_f , b_i , b_c , and b_o are the deviation weights, $t - 1$ is the previous time state, t represents the current time state, x_t is the input vector, and h_t represents the output vector. Here, f_t acts as the forget gate and decides what past PM_{2.5} information and other factors should be forgotten from the cell state. i_t expresses the input gate, which makes the decision on what new data to store in the cell state. Lastly, \tilde{C}_t is a self-recurrent cell in a neuron, and C_t is the LSTM block's internal memory cell.

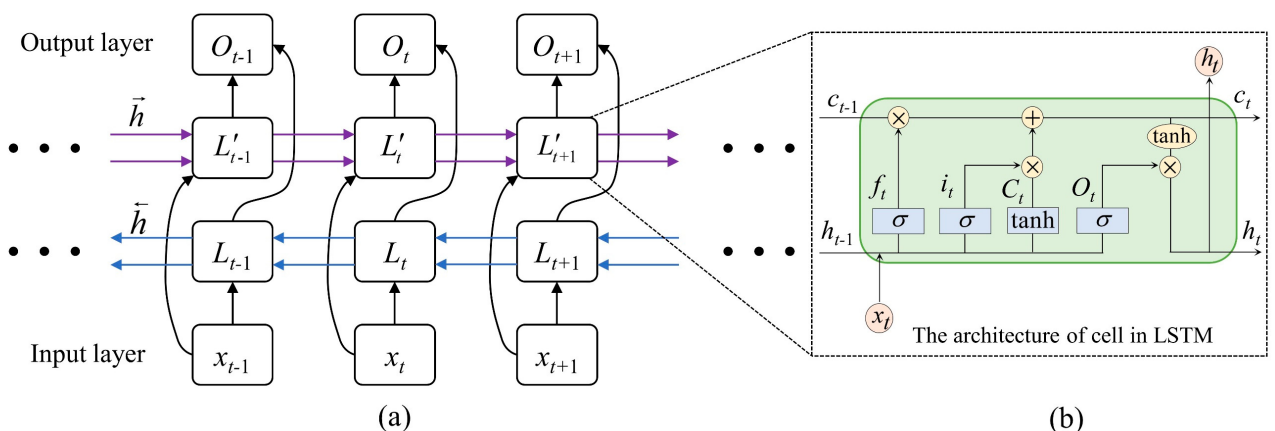


Figure 5. The basic structure of the Bi LSTM. (a) The Bi LSTM. (b) The basic structure of LSTM.

The Bi LSTM model, as shown in Figure 5, in contrast to the LSTM model, is made up of a forward LSTM layer \vec{h} and a backward LSTM layer \overleftarrow{h} . Due to the separate hidden layers in both directions, the Bi LSTM can analyze sequence data in both forward and backward directions. Each hidden layer enables the recording of information from the past (forward) and the future (backward) [36]. As a result, a more thorough collection of PM_{2.5} characteristics may be retrieved to raise the network's prediction accuracy.

2.3. Experimental Setup

In this experiment, we use Keras based on Tensorflow to construct comparative models of deep learning (CNN, LSTM, Bi LSTM, and CNN-LSTM) and the proposed CBAM-CNN-Bi LSTM model. Table 2 displays the parameters utilized to train the prediction model. Then, we use Adam (adaptive gradient algorithm) as the optimization algorithm and MSE as the loss function for the prediction model. In addition, to enhance the model's capacity for generalization, we packaged the dataset and broke it up, splitting the dataset so that the training set contains 80% of the dataset and the test set contains 20%.

Table 2. CBAM-CNN-Bi LSTM model parameters setting.

Parameters	Value
Kernel size of CNN	3×3
Convolution channels	32
Convolution layer	1
Bi LSTM nodes	128
Bi LSTM layer	1
Fully connected layer nodes	12
Fully connected layer	1
Learning rate	0.0001
Batch size	128
Epochs	50

3. Results and Discussion

3.1. Performance Evaluation Indices

This paper uses RMSE, MAE, R^2 , and IA to analyze how well the prediction models performed. The RMSE reflects the sensitivity of the model to error, and the MAE reflects the stability of the model; the closer the value of both to 0, the better the prediction result. R^2 represents the ability to forecast the actual data, and IA represents the similarity of the distribution between actual and predicted values, both variables' values span from [0, 1], the closer to 1, the more consistent the predicted results are with the distribution of the true data. The calculation formula is shown as shown.

$$\text{RMSE} = \sqrt{\frac{1}{n} \sum_{i=1}^n (y_i - \hat{y}_i)^2} \quad (13)$$

$$\text{MAE} = \frac{1}{n} \sum_{i=1}^n |y_i - \hat{y}_i| \quad (14)$$

$$R^2 = \frac{\sum_{i=1}^n (\hat{y}_i - \bar{y})^2}{\sum_{i=1}^n (y_i - \bar{y})^2} \quad (15)$$

$$IA = 1 - \frac{\sum_{i=1}^n (y_i - \hat{y}_i)^2}{\sum_{i=1}^n (|y_i - \bar{y}| + |\hat{y}_i - \bar{y}|)^2} \quad (16)$$

where n denotes the sample size in the dataset, \hat{y}_i denotes predicted value corresponding to it, y_i denotes actual concentration of PM_{2.5}, and \bar{y} represents the mean of all measurements of PM_{2.5} concentrations.

3.2. Correlation Analysis of Variables

In this subsection, we correlated PM_{2.5} concentrations to achieve two objectives. First, we investigate the relationships between PM_{2.5} concentrations, pollutant concentrations, and meteorological data. Furthermore, to ensure the convergence of the model, we placed the highly correlated factors of influence in the same channel. The correlations between the 12 variables in all sites are shown in Figure 6. For absolute values of correlation, among the pollutants, the highest correlation between PM_{2.5} and itself was found, with PM₁₀ (0.89), CO (0.80), NO₂ (0.67), SO₂ (0.39), and O₃ following (-0.17). Among the meteorological factors, wind speed (-0.29) had the strongest association with PM_{2.5}, followed by temperature (-0.15) and dew point (0.11). The absolute values of the correlation coefficients for all other influences were below 0.1. In this paper, the six influential factors with the highest absolute values of correlation coefficients with PM_{2.5} are put into the same channel; they are PM_{2.5}, PM₁₀, CO, NO₂, SO₂, and wind speed. We put O₃ (-0.17), temperature, pressure, dew

point, precipitation, and wind direction into another channel of the model input, forming a 12*6*2 “image”.

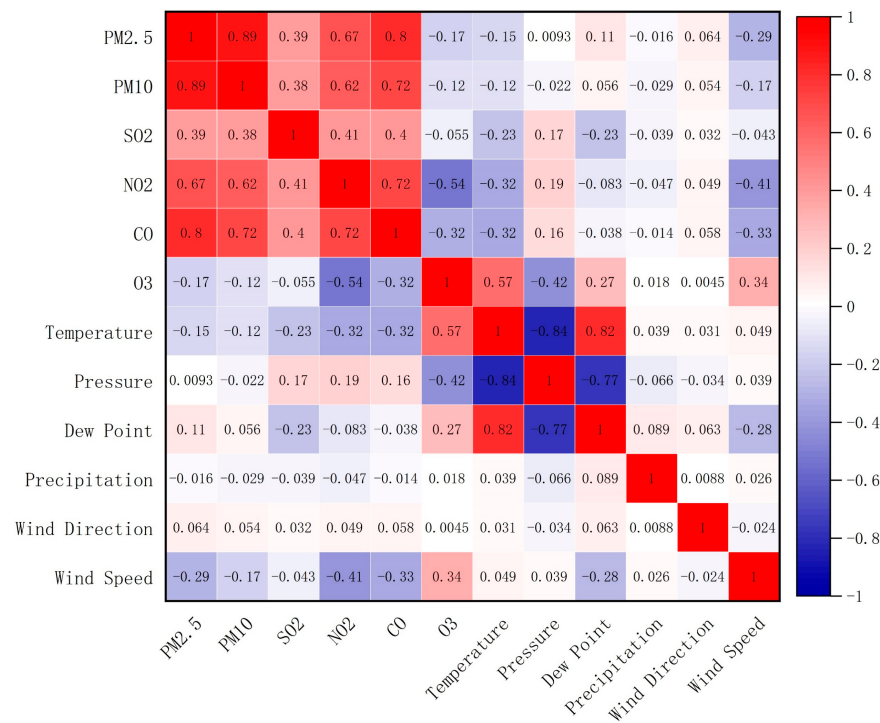


Figure 6. Correlation result of multiple variables.

In terms of pollutants, PM_{2.5} concentrations have a highly substantial association with PM₁₀, CO, NO₂, and SO₂, and a bad relationship with O₃ concentrations. This is due to the fact that PM_{2.5}, PM₁₀, CO, NO₂, and SO₂ are mostly derived from human activities such as coal combustion, vehicle exhausts, and industrial manufacturing. In addition, emissions of PM₁₀, CO, NO₂, and SO₂ contribute to a certain extent to the increase in PM_{2.5} concentrations. Unlike other pollutants, O₃ comes mainly from nature. As light and temperature increase, the concentration of O₃ increases. Due to the high concentration of O₃, there is a chance that some photochemical reactions will consume some PM_{2.5} and lower its concentration.

Compared to pollutants, meteorological factors have a relatively small but integral impact on PM_{2.5} concentrations. The relationship between wind speed and PM_{2.5} concentrations is negative. High wind speeds are conducive to PM_{2.5} dispersion and therefore have a substantial impact on the concentration of PM_{2.5}. The increase in temperature causes instability in the atmosphere, which has a positive effect on the dispersion of PM_{2.5}. The dew point, a measure of air humidity, is positively correlated with PM_{2.5} concentrations. An environment with high air humidity contributes to the formation of fine particulate matter, making PM_{2.5} less likely to disperse. Wind direction, barometric pressure, and rainfall are all weakly correlated with PM_{2.5} and their changes have little effect on PM_{2.5} concentrations.

3.3. Short-Term Prediction

Pollutant prediction models can be divided into short-term prediction models and long-term prediction models [37]. Short-term prediction focuses on the accuracy of the forecast and ensures the safety of human activities in the short term by keeping the forecast time within 12 h [38]. We will compare and analyze the short-term prediction performance of each model for pollutant concentrations in this section.

3.3.1. Effect of Convolution Kernel Size on Experimental Results

The convolutional kernel is a key part of the convolutional neural network model, which directly affects how well the features are extracted and how quickly the network converges. The size of the convolution kernel should be appropriate to the size of the input “image”. If the convolution kernel is too large, the local features cannot be extracted effectively; if the convolution kernel is too small, the overall features cannot be extracted successfully. Therefore, a convolution kernel of the right size should be selected to fit the input “image”. As the size of the input “image” of the CBAM-CNN-Bi LSTM model is $12 \times 6 \times 2$, we set the convolution kernel to 2×2 , 3×3 , 4×4 , 5×5 to forecast the $\text{PM}_{2.5}$ concentrations in the next 6 h.

Table 3 gives the average of the performance evaluation indicators of the CBAM-CNN-Bi LSTM for $\text{PM}_{2.5}$ concentration prediction for the next 6 h at different convolutional kernel sizes. As shown in Table 3, the test errors of the models do not differ significantly when the size of the convolution kernel varies. However, when the convolutional kernel size was 3×3 , RMSE and MAE reached a minimum value of 29.65 and 18.58, and R^2 and IA reached a maximum value of 0.8192 and 96.01%.

Table 3. Effect of convolution kernel size on experimental results in CBAM-CNN-Bi LSTM. (RMSE is the root mean squared error, MAE is the mean squared error, R^2 is the r-squared, IA is the index of agreement).

Convolution Kernel Size	RMSE	MAE	R^2	IA
2×2	29.79	18.84	0.8153	95.92%
3×3	29.65	18.58	0.8192	96.01%
4×4	30.26	19.12	0.8141	95.82%
5×5	30.14	18.83	0.8162	95.85%

Note: window size = 6 (the model’s input window size represents historical observations), and model performance evaluation indicators (RMSE, MAE, R^2 and IA) are the average of prediction of the next 1–6 h.

This demonstrates that the highest prediction performance for our proposed model occurs when the convolution kernel is 3×3 . When the convolution kernel is smaller than 3×3 , the model has an underfitting problem for the overall spatial features of $\text{PM}_{2.5}$ concentrations; when the size of the kernel is larger than 3×3 , our model cannot effectively extract the local spatial features of $\text{PM}_{2.5}$ concentrations. When the convolution kernel is 3×3 , the model is capable of extracting both global and local spatial information related to $\text{PM}_{2.5}$ concentrations. In the following experiments, the convolution kernel size is set to 3×3 .

3.3.2. Effect of Different Models on Experimental Results

The quantitative results for single-step $\text{PM}_{2.5}$ concentrations prediction are given in Table 4, which gives a comparison of the RMSE, MAE, R^2 and IA for CNN, LSTM, Bi LSTM, CNN-LSTM and CBAM-CNN-Bi LSTM. As shown in Table 4, our proposed model performed better than other deep learning models in single-step $\text{PM}_{2.5}$ concentration prediction. In contrast to other models, our proposed model has the minimum prediction error and the greatest prediction accuracy and reduces RMSE to 18.90, MAE to 11.20, improves R^2 to 0.9397, and IA to 98.54%. However, the prediction results of our proposed model are not much ahead of Bi LSTM because the single-step prediction is relatively simple and does not reflect the advantages of our designed architecture. In addition, CNN has the worst prediction performance, and LSTM and Bi LSTM perform predictions more accurately than CNN-LSTM. This means that the LSTM and Bi LSTM, with their excellent time series data processing capability, are more suitable than CNN-LSTM for the $\text{PM}_{2.5}$ concentration single-step prediction task.

Table 4. Performance evaluation indicators for model single-step prediction.

Models	RMSE	MAE	R ²	IA
CNN	23.15	14.15	0.9136	97.83%
LSTM	19.53	11.49	0.9314	98.39%
Bi LSTM	18.94	11.35	0.9370	98.30%
CNN-LSTM	20.51	11.99	0.9313	98.31%
CBAM-CNN-Bi LSTM	18.90	11.20	0.9397	98.54%

Note: window size = 3, and model performance evaluation indicators (RMSE, MAE, R² and IA) are the prediction of the next 1 h.

It is well known that with the increase in forecast time steps, forecasting becomes more difficult. To further evaluate the PM_{2.5} concentrations short-term prediction capability of CBAM-CNN-Bi LSTM and other deep learning models, we predicted PM_{2.5} concentrations for the next 2–12 h and presented the predicted quantitative results through the change curves of RMSE, MAE, R² and IA in Figure 7. As shown in Figure 7, the predictive ability of all prediction models declines as the prediction time step rises. We observed that four performance evaluation indicators of CNN were always worse than other deep learning models, and the LSTM and Bi LSTM prediction performance was generally consistent. Interestingly, as shown in Figure 7a,b, in cases where the predicted time step is under five, compared to the LSTM and Bi LSTM, the CNN-LSTM has a greater prediction error. Does this mean that CNN-LSTM has poorer short-term prediction performance than LSTM and Bi LSTM? In fact, we will find that four metrics for evaluating the performance of the CNN-LSTM start to outperform the LSTM and Bi LSTM when the prediction step size is greater than five. This suggests that CNN-LSTM, with its hybrid model structure, can better quantify complex data when prediction problems become difficult. It is worth noting that when prediction time steps are greater than 4, our proposed model consistently maintains optimal prediction performance with the lowest RMSE and MAE, and the highest R² and IA.

In summary, for PM_{2.5} concentrations short-term prediction, when the convolution kernel is 3*3, CBAM-CNN-Bi LSTM obtains the best prediction performance and maintains the best results among all deep learning models. This means that CBAM plays a key role in the prediction of deep learning models. CBAM obtains the feature relationship between pollutant data and meteorological data, optimizes the CNN spatial feature extraction, and improves the model prediction accuracy.

3.4. Long-Term Prediction

The research on pollutant concentration prediction has mainly focused on pollutant concentration short-term prediction, but this is not sufficient to meet the actual demand. The purpose of long-term forecasting is to forecast pollutant concentrations for a longer period of time in the future, and its predictions can serve as a useful reference for managers. It can be seen that long-term predictions of pollutant concentrations are very meaningful. We will analyze the pollutant concentration long-term prediction performance of each model in this section.

3.4.1. PM_{2.5} Concentration Prediction

The quantitative results of the long-term PM_{2.5} concentration prediction (h13~h18) are given in Table 5, which gives the comparison of RMSE, MAE, R², and IA for CNN, LSTM, Bi LSTM, CNN-LSTM, and our proposed model. As shown in Table 5, our proposed model outperforms other deep learning models in PM_{2.5} concentration prediction (h13~h18). In comparison to alternative models, CBAM-CNN-Bi LSTM has the lowest prediction error and the highest prediction accuracy and reduces RMSE to 37.33, MAE to 26.54, R² to 0.6981, and IA to 93.50%. As shown in Table 5, the R² of CNN has decreased to −0.2546, which indicates that CNN is inappropriate for long-term PM_{2.5} concentration prediction. It is worth noting that the prediction performance of CNN-LSTM is superior to Bi LSTM and

LSTM, this shows that the hybrid model of CNN-LSTM is more suitable for long-term PM_{2.5} concentration prediction.

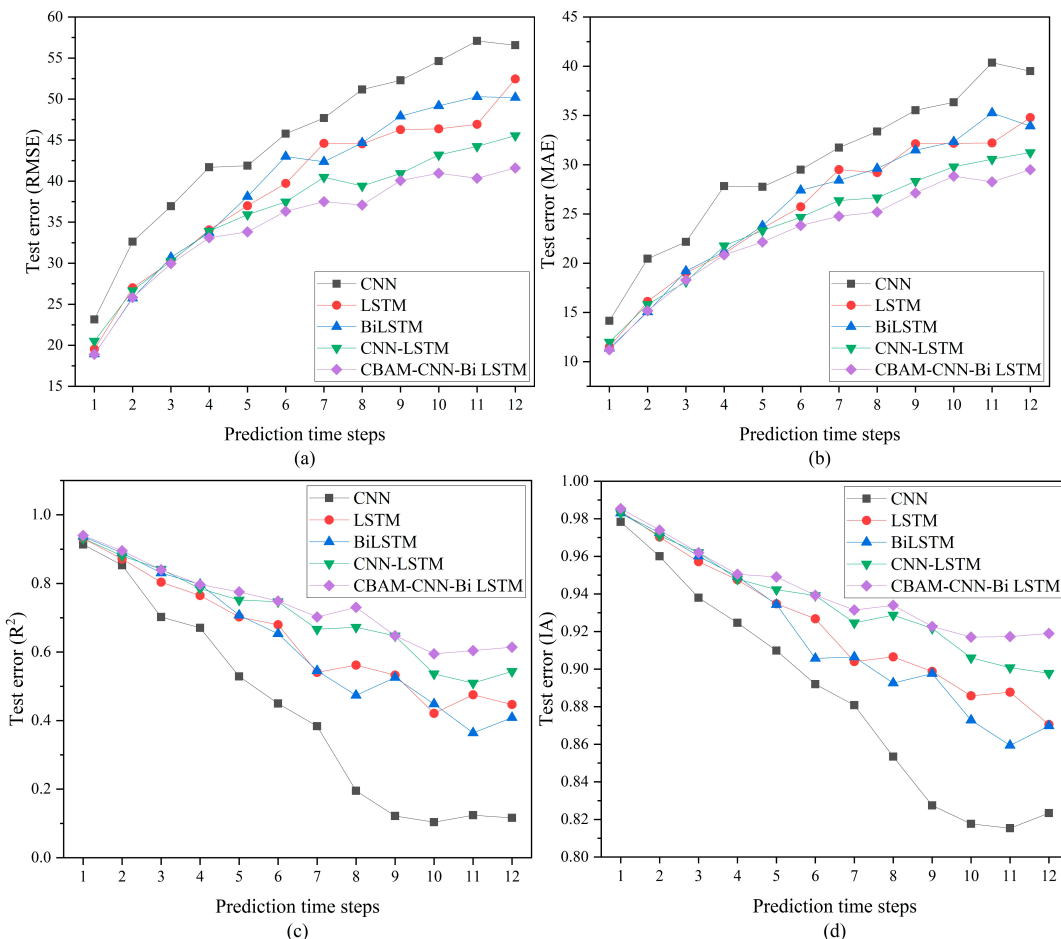


Figure 7. RMSE, MAE, R², and IA of the CBAM-CNN-Bi LSTM model at different prediction time steps and comparisons with other deep learning models. (a) RMSE of models at different prediction steps. (b) MAE of models at different prediction steps. (c) R² of models at different prediction steps. (d) IA of models at different prediction steps.

Table 5. Performance evaluation indicators for model prediction (h13–h18).

Models	RMSE	MAE	R ²	IA
CNN	58.79	41.53	-0.2546	79.05%
LSTM	49.71	34.87	0.3561	87.03%
Bi LSTM	48.84	34.89	0.4132	87.73%
CNN-LSTM	42.84	30.41	0.5876	91.12%
CBAM-CNN-Bi LSTM	37.33	26.54	0.6981	93.50%

Note: window size = 18, and model performance evaluation indicators (RMSE, MAE, R², and IA) are the average of prediction of the next 13–18 h.

Next, we analyze the effect of the size of the prediction time steps on CNN, LSTM, Bi LSTM, CNN-LSTM, and our proposed model. As shown in Tables 6–8, when the prediction time steps are the same as h13~h18, the larger the window size, the more accurate the model's prediction performance. This means that deep learning models can optimize the prediction results by learning more historical data. Table 5 shows that the prediction performance of all deep learning methods steadily declines as prediction step size increases. It is evident that, in contrast to other deep learning methods, our proposed model has the

minimum prediction error (RMSE and MAE) and the highest prediction accuracy (R^2 and IA) for different prediction time steps.

Table 6. Performance evaluation indicators for model prediction (h13–h24).

Models	RMSE		MAE		R^2		IA	
	13–18 h	19–24 h						
CNN	58.53	62.59	42.28	45.33	−0.3338	−1.0071	78.25%	72.26%
LSTM	47.99	52.94	34.54	37.73	0.4216	0.2746	88.06%	85.25%
Bi LSTM	45.42	49.45	32.72	35.57	0.5182	0.3972	89.67%	87.44%
CNN-LSTM	40.30	43.44	28.54	31.45	0.6386	0.5525	92.20%	90.57%
CBAM-CNN-Bi LSTM	34.75	37.00	24.70	26.53	0.7508	0.6942	94.49%	93.49%

Note: window size = 24, and model performance evaluation indicators (RMSE, MAE, R^2 and IA) are the average of prediction of the next $t \sim t + n$ hours.

Table 7. Testing error for model prediction (h13–h48).

Models	RMSE			MAE		
	13–18 h	19–24 h	25–48 h	13–18 h	19–24 h	25–48 h
CNN	57.19	61.82	65.69	40.41	44.63	48.19
LSTM	46.03	48.60	49.34	32.76	35.49	35.90
Bi LSTM	43.07	44.94	45.68	31.05	32.03	33.43
CNN-LSTM	37.20	38.55	40.24	26.51	27.45	29.16
CBAM-CNN-Bi LSTM	31.47	31.84	32.34	21.86	21.78	22.30

Note: window size = 48, and prediction error is averaged out by model testing error (RMSE and MAE). of the future $t \sim t + n$ hours.

Table 8. Testing accuracy for model prediction (h13–h48).

Models	R^2			IA		
	13–18 h	19–24 h	25–48 h	13–18 h	25–36 h	25–48 h
CNN	−0.1841	−0.9108	−1.3622	80.01%	73.68%	68.79%
LSTM	0.5019	0.3845	0.3467	89.44%	87.53%	87.02%
Bi LSTM	0.5538	0.5294	0.4930	90.76%	90.03%	89.50%
CNN-LSTM	0.7190	0.7077	0.6637	93.74%	93.31%	92.52%
CBAM-CNN-Bi LSTM	0.8068	0.8042	0.7980	95.52%	95.50%	95.39%

Note: window size = 48, and model testing accuracy (R^2 and IA) are the average of prediction accuracy of the next $t \sim t + n$ hours.

To verify the effectiveness of our proposed model, we analyzed the variations of RMSE, MAE, R^2 , and IA for each model within the prediction step of 48 h. As shown in Tables 7 and 8, the four performance evaluation indicator metrics of CNN, Bi LSTM, LSTM, and CNN-LSTM fluctuated widely in the long-term prediction. Furthermore, what is interesting about the data in Tables 7 and 8 is that our proposed model can continue to outperform the CNN-LSTM significantly as the prediction time step grows. In addition, the four evaluation indicators of our proposed model fluctuated less (with little change in values) as the prediction time steps increased, which shows that CBAM-CNN-Bi LSTM is most suitable for long-term PM_{2.5} concentration prediction. In conclusion, our proposed model can be used to maintain the best and most stable prediction performance in long-term PM_{2.5} concentration prediction.

To further validate the prediction performance of our proposed model, we analyzed the fitting ability of our proposed model and four other deep learning models for PM_{2.5} concentrations at a prediction time step of 48 h. As shown in Figure 8a1–e1, we found that the CNN has the worst prediction performance and cannot describe the trend of PM_{2.5} concentrations. Compared to LSTM and Bi LSTM, CNN-LSTM has a higher long-term prediction ability for PM_{2.5} concentrations, but the accuracy of the prediction of sudden

change points of PM_{2.5} concentrations is not enough. Our proposed model shown in Figure 8 outperforms other comparative models in the prediction of sudden change points in PM_{2.5} concentrations. We observed that when the PM_{2.5} concentrations were larger than 200 $\mu\text{g}/\text{m}^3$, the comparison model's predicted outcomes were unable to capture the true trend. This also reflects that when the PM_{2.5} concentrations are too high, it makes precise prediction using the model challenging. Moreover, the predictions of our proposed model and the observed outcomes are virtually identical (as shown in the red wireframe part in Figure 8). This means that our proposed model has a good fit for the prediction of high PM_{2.5} concentration values.

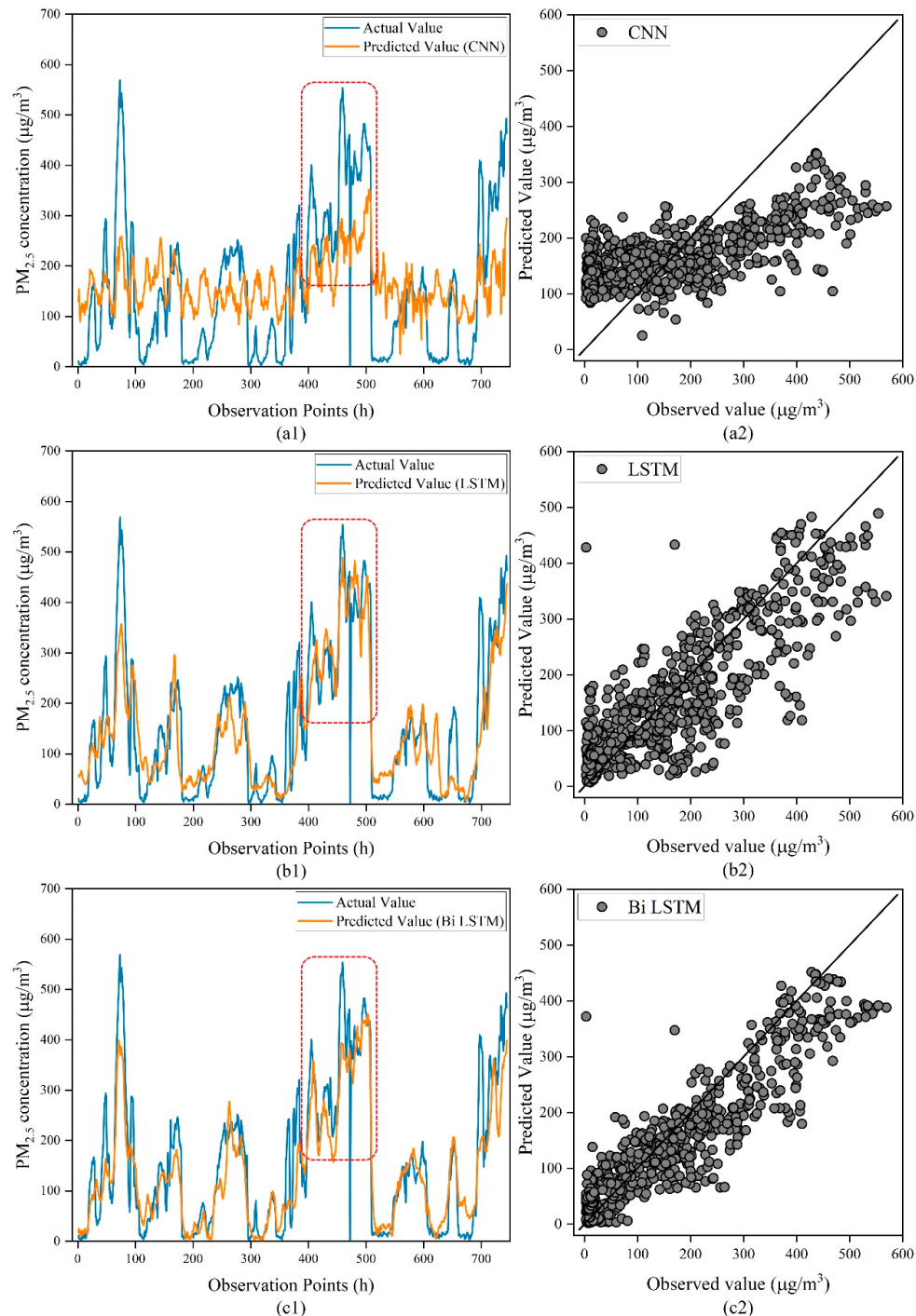


Figure 8. Cont.

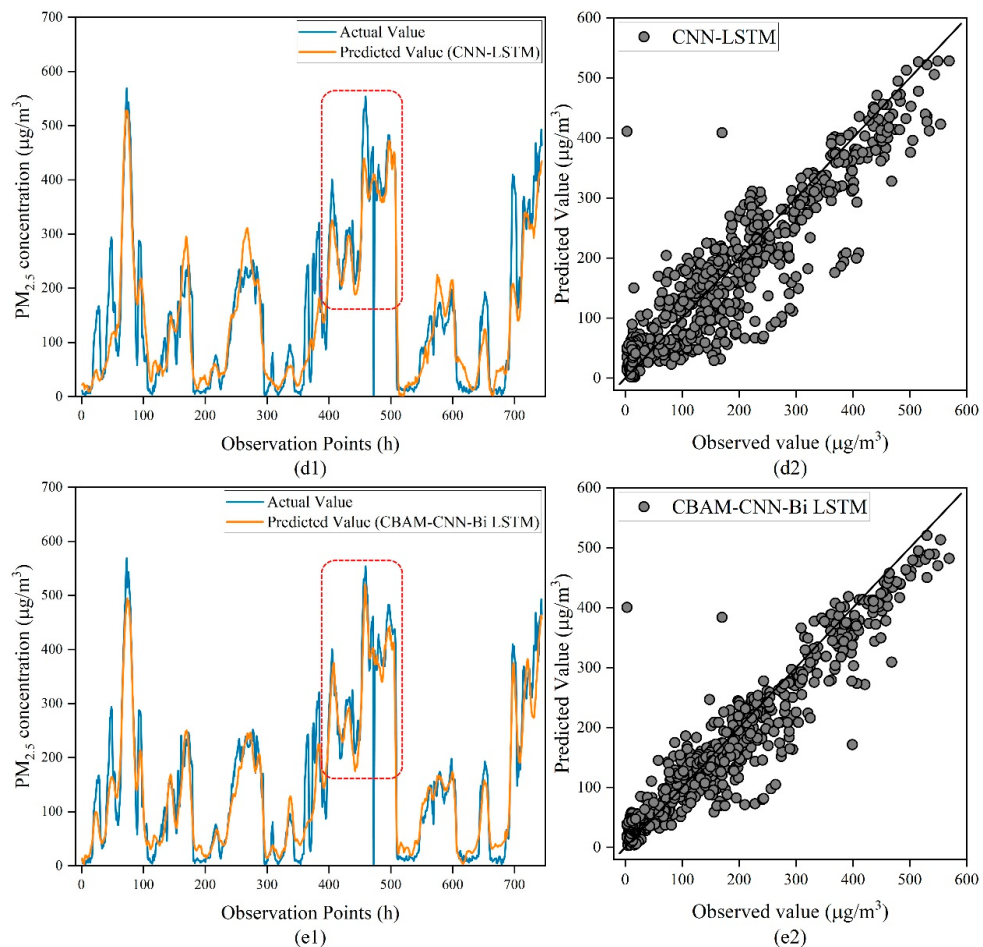


Figure 8. Comparison of PM_{2.5} concentration prediction models for the next 48h at station 1001A. **(a1)** Prediction line graph of CNN model; **(a2)** Prediction scatter plot of CNN model; **(b1)** Prediction line graph of LSTM model; **(b2)** Prediction scatter plot of LSTM model; **(c1)** Prediction line graph of Bi LSTM model; **(c2)** Prediction scatter plot of Bi LSTM model; **(d1)** Prediction line graph of CNN-LSTM model; **(d2)** Prediction scatter plot of CNN-LSTM model; **(e1)** Prediction line graph of CBAM-CNN-Bi LSTM model; **(e2)** Prediction scatter plot of CBAM-CNN-Bi LSTM model.

Combined with the capability of fitting the model in Figure 8, we can draw the following conclusions: (1) CBAM-CNN-Bi LSTM has better prediction performance in all time periods and can effectively forecast PM_{2.5} concentrations in different environments; (2) in the case of high PM_{2.5} concentration values, the CBAM-CNN-Bi LSTM has a good fitting effect, making the predicted and observed values basically consistent; (3) we can see that the number of sudden change point samples is relatively small. This phenomenon causes the deep learning model to insufficiently learn the change pattern of PM_{2.5} concentrations in the case of sudden changes. This is the reason why the deep learning model is difficult to fit to the sudden change points.

3.4.2. Other Pollutant Concentration Prediction

To confirm the applicability of our suggested model. In this section, PM₁₀ and SO₂ are used as examples, and Tables 9 and 10 display the evaluation indices of model prediction performance. As shown in Table 9, our proposed model still has the best prediction ability. The prediction performance of our proposed model is significantly better than that of the single framework model. Compared with the CNN-LSTM model, our proposed model reduces RMSE by 3.57, MAE by 2.65, R² by 0.0115, and IA by 0.59%. This indicates that the convolutional block attention module optimizes the model and improves the prediction accuracy. The predicted results for SO₂ are similar to those for PM₁₀. As shown in Table 10,

our model reduced the RMSE to 9.87, MAE to 6.14, R^2 to 0.7175, and IA to 93.76%. In the prediction of SO_2 and PM_{10} , our model also maintains the optimal prediction results. This indicates that our proposed prediction approach is applicable to the prediction of other pollutants and is as successful.

Table 9. Performance evaluation indicators for model prediction of PM_{10} (h13–h48).

Models	RMSE	MAE	R^2	IA
CNN	73.05	53.15	−1.1639	70.69%
LSTM	56.12	41.12	0.3816	87.19%
Bi LSTM	54.97	40.77	0.4212	88.09%
CNN-LSTM	45.92	32.72	0.6818	92.74%
CBAM-CNN-Bi LSTM	42.35	30.07	0.6933	93.33%

Note: window size = 48, and model performance evaluation indicators (RMSE, MAE, R^2 and IA) are the average of prediction of the next 13–48 h.

Table 10. Performance evaluation indicators for the model prediction of SO_2 (h13–h48).

Models	RMSE	MAE	R^2	IA
CNN	15.19	9.59	−0.0793	80.79%
LSTM	13.54	8.38	0.3172	86.35%
Bi LSTM	13.15	8.22	0.3445	87.11%
CNN-LSTM	11.23	7.05	0.6568	92.53%
CBAM-CNN-Bi LSTM	9.87	6.14	0.7175	93.76%

Note: window size = 48, and model performance evaluation indicators (RMSE, MAE, R^2 , and IA) are the average of prediction of the next 13–48 h.

4. Conclusions and Future

In my research, a unique $\text{PM}_{2.5}$ concentration prediction model (CBAM-CNN-Bi LSTM) is proposed, which gives a reasonable prediction by learning from a large amount of pollutant data and meteorological data. CBAM-CNN-Bi LSTM is a hybrid deep learning model which consists of CBAM, CNN, and Bi LSTM. The advantages of CBAM-CNN-Bi LSTM are concluded as below:

- (1) By utilizing the convolutional block attention module, the CNN network degradation issue may be solved. The spatial attention module assists CNN in efficiently acquiring spatial correlation features between multiple sites to extract pollutants and meteorological data. The channel attention module is used to capture the complex relationship features between the influencing factors of model inputs. Convolutional block attention modules optimize convolutional neural networks to provide more reliable data for more precise result prediction;
- (2) By using Bi LSTM as the output prediction layer, the model not only obtains the performance advantage of long-time series prediction through Bi LSTM, avoiding the problem of underutilization of contextual information, but also extracts the effective association features of the output of the convolutional neural network layer to achieve the goal of mining data spatiotemporal association;
- (3) Our proposed model can be simultaneously applied to meteorological and pollution data from multiple stations for environmental monitoring of big data while considering the changes in the spatial and temporal distribution of the data to achieve the prediction of air pollutant concentrations in the target city. Experiments conducted on the dataset show that our framework obtains better results than other methods.

Based on the aforementioned experimental findings, the effectiveness of our proposed model is demonstrated. In comparison to other models, our proposed model gives accurate $\text{PM}_{2.5}$ concentration predictions by fully extracting the temporal and spatial characteristics of $\text{PM}_{2.5}$ and the correlation between pollutant data and meteorological data and overcoming the problem of long-time dependence of $\text{PM}_{2.5}$ concentrations. Therefore, our proposed

model overcomes the weaknesses of CNN-LSTM and has more practical value. However, traffic, vegetation cover, and pedestrian flow are not considered in this paper, which will be addressed in future studies.

Author Contributions: Conceptualization, D.L.; methodology, D.L.; software, D.L.; validation, D.L.; formal analysis, Y.Z.; investigation, J.L.; resources, J.L.; data curation, D.L.; writing—original draft preparation, D.L.; writing—review and editing, D.L. and Y.Z.; visualization, Y.Z.; supervision, J.L.; project administration, Y.Z.; funding acquisition, Y.Z. All authors have read and agreed to the published version of the manuscript.

Funding: This work was supported by Lanzhou Jiaotong University (grant no. EP 201806).

Institutional Review Board Statement: Not applicable.

Informed Consent Statement: Not applicable.

Data Availability Statement: Restrictions apply to the availability of these data. Data was obtained from [Songxi Chen] and are available [<https://archive.ics.uci.edu/ml/datasets/Beijing+Multi-Site+Air-Quality+Data>] with the permission of [Songxi Chen].

Conflicts of Interest: The authors declare no conflict of interest.

References

1. Fong, I.H.; Li, T.; Fong, S.; Wong, R.K.; Tallon-Ballesteros, A.J. Predicting concentration levels of air pollutants by transfer learning and recurrent neural network. *Knowl.-Based Syst.* **2020**, *192*, 105622. [[CrossRef](#)]
2. Maleki, H.; Sorooshian, A.; Goudarzi, G.; Baboli, Z.; Birgani, Y.T.; Rahmati, M.J. Air pollution prediction by using an artificial neural network model. *Clean Technol. Environ. Policy* **2019**, *21*, 1341–1352. [[CrossRef](#)] [[PubMed](#)]
3. Chen, F.; Chen, Z. Cost of economic growth: Air pollution and health expenditure. *Sci. Total Environ.* **2021**, *755*, 142543. [[CrossRef](#)]
4. Park, S.; Kim, M.; Kim, M.; Namgung, H.G.; Kim, K.T.; Cho, K.H.; Kwon, S.B. Predicting PM10 concentration in Seoul metropolitan subway stations using artificial neural network (ANN). *J. Hazard. Mater.* **2017**, *341*, 75–82. [[CrossRef](#)] [[PubMed](#)]
5. Zhang, B.; Zou, G.; Qin, D.; Ni, Q.; Mao, H.; Li, M. RCL-Learning: ResNet and convolutional long short-term memory-based spatiotemporal air pollutant concentration prediction model. *Expert Syst. Appl.* **2022**, *207*, 118017. [[CrossRef](#)]
6. Djalalova, I.; Delle Monache, L.; Wilczak, J. PM2.5 analog forecast and Kalman filter post-processing for the Community Multiscale Air Quality (CMAQ) model. *Atmos. Environ.* **2015**, *108*, 76–87. [[CrossRef](#)]
7. Zhu, B.; Akimoto, H.; Wang, Z. The Preliminary Application of a Nested Air Quality Prediction Modeling System in Kanto Area, Japan. *AGU Fall Meet. Abstr.* **2005**, *2005*, A33F-08.
8. Saide, P.E.; Carmichael, G.R.; Spak, S.N.; Gallardo, L.; Osses, A.E.; Mena-Carrasco, M.A.; Pagowski, M. Forecasting urban PM10 and PM2.5 pollution episodes in very stable nocturnal conditions and complex terrain using WRF-Chem CO tracer model—ScienceDirect. *Atmos. Environ.* **2011**, *45*, 2769–2780. [[CrossRef](#)]
9. Zou, G.; Zhang, B.; Yong, R.; Qin, D.; Zhao, Q. FDN-learning: Urban PM 2.5-concentration Spatial Correlation Prediction Model Based on Fusion Deep Neural Network. *Big Data Res.* **2021**, *26*, 100269. [[CrossRef](#)]
10. Rubal; Kumar, D. Evolving Differential evolution method with random forest for prediction of Air Pollution. *Procedia Comput. Sci.* **2018**, *132*, 824–833. [[CrossRef](#)]
11. Zhang, H.; Zhang, S.; Wang, P.; Qin, Y.; Wang, H. Forecasting of particulate matter time series using wavelet analysis and wavelet-ARMA/ARIMA model in Taiyuan, China. *J. Air Waste Manag. Assoc.* **2017**, *67*, 776–788. [[CrossRef](#)] [[PubMed](#)]
12. Zhang, L.; Lin, J.; Qiu, R.; Hu, X.; Zhang, H.; Chen, Q.; Tan, H.; Lin, D.; Wang, J. Trend analysis and forecast of PM2.5 in Fuzhou, China using the ARIMA model. *Ecol. Indic.* **2018**, *95*, 702–710. [[CrossRef](#)]
13. Leong, W.; Kelani, R.; Ahmad, Z. Prediction of air pollution index (API) using support vector machine (SVM). *J. Environ. Chem. Eng.* **2019**, *8*, 103208. [[CrossRef](#)]
14. Yu, Z.; Yi, X.; Ming, L.; Li, R.; Shan, Z. Forecasting Fine-Grained Air Quality Based on Big Data. In Proceedings of the the 21th ACM SIGKDD International Conference, Sydney, Australia, 10–12 August 2015.
15. Huang, C.-J.; Kuo, P.-H. A Deep CNN-LSTM Model for Particulate Matter (PM2.5) Forecasting in Smart Cities. *Sensors* **2018**, *18*, 2220. [[CrossRef](#)] [[PubMed](#)]
16. Yang, J.; Yan, R.; Nong, M.; Liao, J.; Li, F.; Sun, W. PM 2.5 concentrations forecasting in Beijing through deep learning with different inputs, model structures and forecast time. *Atmos. Pollut. Res.* **2021**, *12*, 101168. [[CrossRef](#)]
17. Xin, R.B.; Jiang, Z.F.; Li, N.; Hou, L.J. *An Air Quality Predictive Model of Licang of Qingdao City Based on BP Neural Network*; Trans Tech Publications Ltd.: Stafa-Zurich, Switzerland, 2012.
18. Fan, J.; Li, Q.; Hou, J.; Feng, X.; Karimian, H.; Lin, S. A Spatiotemporal Prediction Framework for Air Pollution Based on Deep RNN. *ISPRS Ann. Photogramm. Remote Sens. Spat. Inf. Sci.* **2017**, *4*, 15. [[CrossRef](#)]
19. Chung, J.; Gulcehre, C.; Cho, K.H.; Bengio, Y. Empirical Evaluation of Gated Recurrent Neural Networks on Sequence Modeling. *arXiv* **2014**, arXiv:1412.3555.

20. Li, X.; Peng, L.; Yao, X.; Cui, S.; Hu, Y.; You, C.; Chi, T. Long short-term memory neural network for air pollutant concentration predictions: Method development and evaluation. *Environ. Pollut.* **2017**, *231*, 997–1004. [[CrossRef](#)]
21. Prihatno, A.T.; Nurcahyanto, H.; Ahmed, M.F.; Rahman, M.H.; Alam, M.M.; Jang, Y.M. Forecasting PM2.5 Concentration Using a Single-Dense Layer BiLSTM Method. *Electronics* **2021**, *10*, 1808. [[CrossRef](#)]
22. Hu, X.; Liu, T.; Hao, X.; Lin, C. Attention-based Conv-LSTM and Bi-LSTM networks for large-scale traffic speed prediction. *J. Supercomput.* **2022**, *78*, 12686–12709. [[CrossRef](#)]
23. Yan, R.; Liao, J.; Yang, J.; Sun, W.; Nong, M.; Li, F. Multi-hour and multi-site air quality index forecasting in Beijing using CNN, LSTM, CNN-LSTM, and spatiotemporal clustering. *Expert Syst. Appl.* **2020**, *169*, 114513. [[CrossRef](#)]
24. Zhao, J.; Deng, F.; Cai, Y.; Chen, J. Long short-term memory—Fully connected (LSTM-FC) neural network for PM 2.5 concentration prediction. *Chemosphere* **2019**, *220*, 486–492. [[CrossRef](#)] [[PubMed](#)]
25. Li, S.; Xie, G.; Ren, J.; Guo, L.; Yang, Y.; Xu, X. Urban PM2.5 Concentration Prediction via Attention-Based CNN-LSTM. *Appl. Sci.* **2020**, *10*, 1953. [[CrossRef](#)]
26. Zhou, Q.; Jiang, H.; Wang, J.; Zhou, J. A hybrid model for PM2.5 forecasting based on ensemble empirical mode decomposition and a general regression neural network. *Sci. Total Environ.* **2014**, *496*, 264–274. [[CrossRef](#)]
27. Qi, Y.; Li, Q.; Karimian, H.; Liu, D. A hybrid model for spatiotemporal forecasting of PM2.5 based on graph convolutional neural network and long short-term memory. *Sci. Total Environ.* **2019**, *664*, 1–10. [[CrossRef](#)]
28. Shi, X.; Chen, Z.; Wang, H.; Yeung, D.Y.; Wong, W.K.; Woo, W.C. Convolutional LSTM Network: A Machine Learning Approach for Precipitation Nowcasting. *Adv. Neural Inf. Process. Syst.* **2015**, *28*, 802–810.
29. Liang, Z.; Zhu, G.; Shen, P.; Song, J. Learning Spatiotemporal Features Using 3DCNN and Convolutional LSTM for Gesture Recognition. In Proceedings of the 2017 IEEE International Conference on Computer Vision Workshops (ICCVW), Venice, Italy, 22–29 October 2017.
30. Liang, Y.; Lin, Y.; Lu, Q. Forecasting gold price using a novel hybrid model with ICEEMDAN and LSTM-CNN-CBAM. *Expert Syst. Appl.* **2022**, *206*, 117847. [[CrossRef](#)]
31. Qin, D.; Yu, J.; Zou, G.; Yong, R.; Zhao, Q.; Zhang, B. A Novel Combined Prediction Scheme Based on CNN and LSTM for Urban PM2.5 Concentration. *IEEE Access* **2019**, *7*, 20050–20059. [[CrossRef](#)]
32. Ma, K.; Zhan, C.a.A.; Yang, F. Multi-classification of arrhythmias using ResNet with CBAM on CWGAN-GP augmented ECG Gramian Angular Summation Field. *Biomed. Signal Process. Control* **2022**, *77*, 103684. [[CrossRef](#)]
33. Woo, S.; Park, J.; Lee, J.Y.; Kweon, I.S. CBAM: Convolutional Block Attention Module. *arXiv* **2018**, arXiv:1807.06521.
34. Wang, Y.; Zhang, Z.; Feng, L.; Ma, Y.; Du, Q. A new attention-based CNN approach for crop mapping using time series Sentinel-2 images—ScienceDirect. *Comput. Electron. Agric.* **2021**, *184*, 106090. [[CrossRef](#)]
35. Krizhevsky, A.; Sutskever, I.; Hinton, G.E. ImageNet Classification with Deep Convolutional Neural Networks. *Commun. ACM* **2017**, *60*, 84–90. [[CrossRef](#)]
36. Du, S.; Li, T.; Yang, Y.; Horng, S.J. Deep Air Quality Forecasting Using Hybrid Deep Learning Framework. *IEEE Trans. Knowl. Data Eng.* **2018**, *33*, 2412–2424. [[CrossRef](#)]
37. Wang, Z.B.; Fang, C.L. Spatial-temporal characteristics and determinants of PM2.5 in the Bohai Rim Urban Agglomeration. *Chemosphere* **2016**, *148*, 148–162. [[CrossRef](#)] [[PubMed](#)]
38. Zhou, J.; Li, W.; Yu, X.; Xu, X.; Yuan, X.; Wang, J. Elman-Based Forecaster Integrated by AdaboostAlgorithm in 15 min and 24 h ahead Power OutputPrediction Using PM 2.5 Values, PV ModuleTemperature, Hours of Sunshine, and Meteorological Data. *Pol. J. Environ. Stud.* **2019**, *28*, 1999. [[CrossRef](#)]